PHOTONIC SENSORS / Vol. 7, No. 1, 2017: 37–43

Study of All-Optical Sampling Using a Semiconductor Optical Amplifier

Chen WU, Yongjun WANG*, Lina WANG, and Fu WANG

School of Electronic Engineering, Beijing University of Posts and Telecommunications, Beijing, 100876, China

*Corresponding author: Yongjun WANG E-mail: wangyj@bupt.edu.cn

Abstract: All-optical sampling is an important research content of all-optical signal processing. In recent years, the application of the semiconductor optical amplifier (SOA) in optical sampling has attracted lots of attention because of its small volume and large nonlinear coefficient. We propose an optical sampling model based on nonlinear polarization rotation effect of the SOA. The proposed scheme has the advantages of high sampling speed and small input pump power, and a transfer curve with good linearity was obtained through simulation. To evaluate the performance of sampling, we analyze the linearity and efficiency of sampling pulse considering the impact of pulse width and analog signal frequency. We achieve the sampling of analog signal to high frequency pulse and exchange the positions of probe light and pump light to study another sampling.

Keywords: All-optical sampling; semiconductor optical amplifier; nonlinear polarization rotation

Citation: Chen WU, Yongjun WANG, Lina WANG, and Fu WANG, "Study of All-Optical Sampling Using a Semiconductor Optical Amplifier," *Photonic Sensors*, 2017, 7(1): 37–43.

1. Introduction

In recent years, the all-optical signal processing system has become a hot research field of optical communication, and it is generally achieved by nonlinear effects of nonlinear elements, in which the semiconductor optical amplifier (SOA) is an important device. On the one hand, the SOA can achieve online amplification in the optical communication link to make up line loss; on the other hand, it has advantages of high nonlinear coefficient, compact structure, low power consumption, and ease to integrate. In particular, the SOA can produce many optical nonlinear effects, such as cross phase modulation (XPM) [1, 2], cross gain modulation (XGM) [3, 4], four-wave mixing (FWM) [5, 6], and nonlinear polarization potation (NPR) [7, 8], which can achieve wavelength conversion, optical switch, optical buffer, and all-optical sampling in the signal processing [9−12]. Compared with other nonlinear effects of the SOA, NPR is applied to more various aspects due to that it is high-speed and easy to implement, and can also achieve a positive and inverted beam at the same time. Since 1990s, the SOA has attracted extensive attention in the study of all-optical signal processing, and its application methods and scope are growing steadily.

2. Working principle

The NPR effect of the SOA is an important aspect of its nonlinear characteristics. The polarization-related characteristics of the SOA include polarization dependent gain (PDG) and

Received: 25 May 2016 / Revised: 10 June 2016

DOI: 10.1007/s13320-016-0354-4
Article type: Regular

polarization dependent phase, resulting in that SOA's output polarization state changes as the input signal. PDG characteristic means that the gains of the transverse electric (TE) mode and transverse magnetic (TM) mode are different, polarization dependent phase characteristic refers to that there is birefringence between the TE and TM modes in the SOA, which leads to that phase change is not the same in two modes after the input light passes through the SOA.

Ignoring the influence of surface remaining reflectance and spontaneous emission, the transmission equations of SOA's photon density and phase in the TE and TM directions are

$$\frac{\partial S^i(z,t)}{\partial z}=\left[\Gamma^i g^i(z,t)-\alpha_{\text{int}}^i\right]S^i,\ \ i=\text{TE or TM} \quad (1)$$

$$\frac{\partial \phi^i(z,t)}{\partial z}=-\frac{1}{2}\alpha^i\Gamma^i g^i(z,t),\ \ i=\text{TE or TM} \quad (2)$$

where Γ is the mode field limiting factor, α is the linewidth enhancement factor (LEF), $g(z,t)$ is the gain, and α_{int} the is mode loss.

The relationship between the photon density S and input light power P is

$$S^i=\frac{P^i}{\hbar\omega}\frac{L}{\upsilon_g},\ \ i=\text{TE or TM}. \quad (3)$$

The gains $g^{\text{TE}}(z,t)$ and $g^{\text{TM}}(z,t)$ are

$$g^{\text{TE}}(z,t)=\xi^{\text{TE}}\left[n_c(z,t)+n_x(z,t)-N_0\right]/V_a \quad (4)$$

$$g^{\text{TM}}(z,t)=\xi^{\text{TM}}\left[n_c(z,t)+n_y(z,t)-N_0\right]/V_a. \quad (5)$$

We introduce the non-equilibrium factor f to measure the anisotropy of the SOA, so the carrier rate equations of TE and TM modes are

$$\frac{\partial n_x(z,t)}{\partial t}=-\frac{n_x(z,t)-\overline{n_x}}{T_1}-\frac{n_x(z,t)-fn_y(z,t)}{T_2}-g^{\text{TE}}(z,t)S^{\text{TE}}(z,t) \quad (6)$$

$$\frac{\partial n_y(z,t)}{\partial t}=-\frac{n_y(z,t)-\overline{n_y}}{T_1}-\frac{fn_y(z,t)-n_x(z,t)}{T_2}-g^{\text{TM}}(z,t)S^{\text{TM}}(z,t) \quad (7)$$

where at equilibrium,

$$\overline{n_{\text{x}}}=\frac{\bar{n}f}{1+f},\ \overline{n_{\text{y}}}=\frac{\bar{n}}{1+f},\ \bar{n}=\frac{I}{e}T_1. \quad (8)$$

As shown in Fig. 1, the proposed optical sampling scheme is based on the NPR effect of the SOA. The optical sampling switch is constituted by the SOA, polarization controller (PC), isolator, circulator, polarizing beam splitter (PBS), and band pass filter (BPF). A narrow Gaussian pulse sequence is used as a probe light, and a sinusoidal optical signal of different wavelengths from probe light is used as a pump light. When PC1 is adjusted to make the input light polarization state be at 45° with SOA's horizontal direction, then PC2 is adjusted to make that there is no effect of the pump light, so that the probe light can have its minimum output through the PBS.

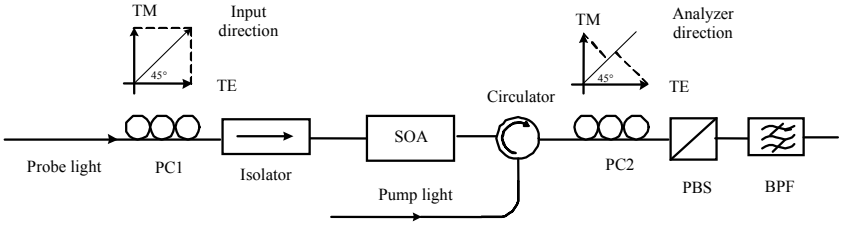

Fig. 1 All-optical sampling scheme based on the NPR effect of the SOA.

3. Simulation results and analysis

3.1 Optical switch performance

For all-optical sampling utilizing the NPR effect, its transfer curve linearity of the PBS port is the key factor that influences the efficiency of the sampling system. To obtain a transfer curve with a good linearity, we analyze the static output curve of 0.1 mW, 0.3 mW, 0.5 mW, 0.7 mW, and 0.9 mW probe lights, the bias current is 350 mA, as shown in

Fig. 2(a). It is observed that the linearity and sampling scopes of 0.1 mW and 0.9 mW are both bad, the sampling scopes of 0.5 mW and 0.7 mW are large, but their linearity is not as good as 0.3 mW, therefore, in the subsequent analysis of the optical sampling application, the probe light power is set to 0.3 mW.

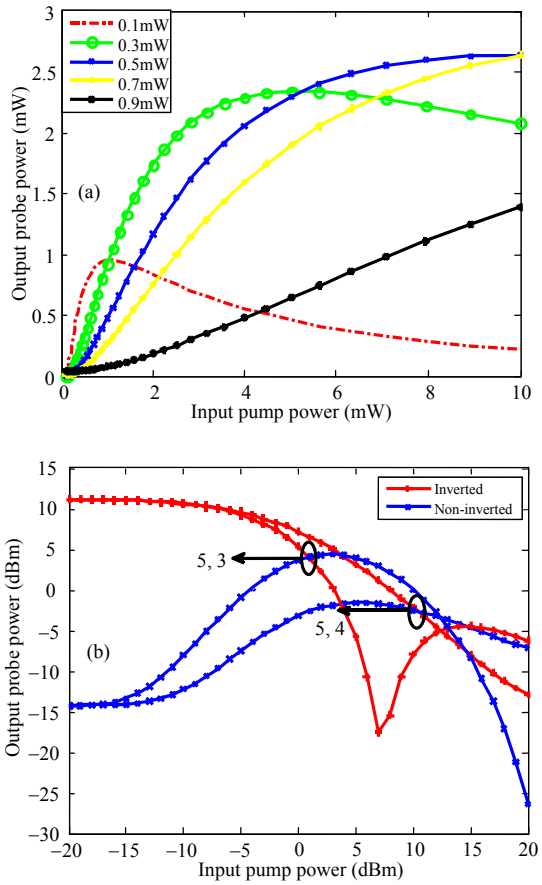

Fig. 2 Output power with respect to the pump power: (a) input probe light power and (b) linewidth enhancement factor.

The probe light passes through the SOA and outputs from the PBS. Static output results of the PBS port are analyzed in Fig 2(b). It can be seen from two non-inverted output curves of the PBS that there is a transfer curve with a good linearity which can be applied to the research on optical sampling. For the curve whose LEFs are 5 and 3, the polarization state is rotated when the pump power is 7 dBm, so it can achieve the polarization optical switch. While another group of curves with small linewidth gain difference, the phase difference is hard to reach π, so it cannot achieve the polarization optical switch even though the pump power is 15 dBm.

3.2 Phase difference factors

Variable curves of phase difference between the TE and TM modes with respect to the bias current, pump power, and probe power are acquired. Figure 3(a) shows the phase difference change with the SOA bias current in the NPR process. With an increase in the bias current, the phase difference increases and becomes saturated, and at the same bias current, when the probe light power is greater, the phase difference is smaller. Figure 3(b) analyzes the phase difference change with the pump light power at different bias currents of different probe light powers. It can be seen from the three groups of curves that when the probe light power is bigger, the phase difference at the same pump power is smaller and easier to saturate. Electrically and optically controlled optical switches can be realized by making the phase difference to π through the appropriate choice of the probe power, pump power, and bias current.

In addition, the impacts of the PDG and LEF on the phase difference are discussed, respectively. The results show that the PDG can affect the phase difference change, but its role is limited. LEF difference is the major influencing factor, and the selection of the SOA with the larger LEF difference can obtain the smaller pump light power to achieve optical sampling. As shown in Fig. 3(c), its maximum phase difference change with the pump power is less than 1 rad by comparing several curves of the PDG from 0.6 dB to 4 dB. Figure 3(d) analyzes effects of different PDGs and LEFs on the phase difference change. It is obvious that when α^{TE} and α^{TM} are 5 and 3, it is still able to reach π phase difference of the 0.6-dB PDG, but it is difficult for other two curves no matter how much the PDG is.

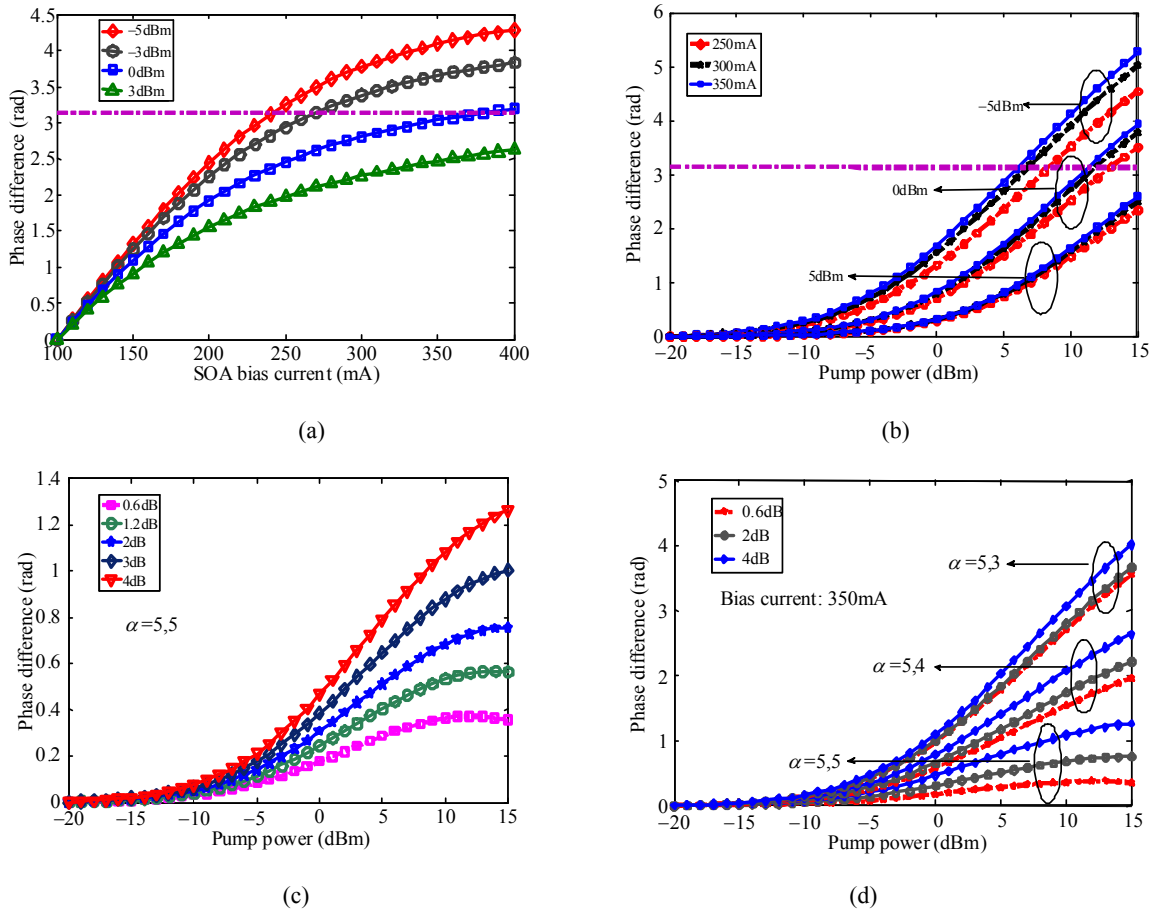

Fig. 3 Curves of phase difference: (a) with bias current and probe power, (b) with pump power, probe power, and bias current, (c) with PDG and pump power, and (d) with PDG, LEF, and pump power.

3.3 Sampling results

We establish an ultrafast all-optical sampling scheme by analyzing SOA's NPR effect, in which the input probe light is a narrow Gaussian pulse sequence, and the input pump light is an analog cosine signal with different wavelengths from the probe light. In the process of optical sampling, the incident pump light modulates the carrier density and gain of the SOA to rotate the polarization state of sampling pulse light, and the polarization state modulation is converted to the intensity modulation through the PBS. The BPF filters analog signal, so that only the ultrafast pulse-modulated light can pass through, and the all-optical sampling is achieved.

Figures 4(a) and 4(b) are the normalized powers of the input probe light and pump light, and the corresponding power curves of the output probe light and their pulse envelopes are shown in Figs. 4(c) and 4(d), respectively. It can be seen from the figures that the information of the analog signal is modulated to the output pulse envelope well, so the sampling of the analog signal to high frequency

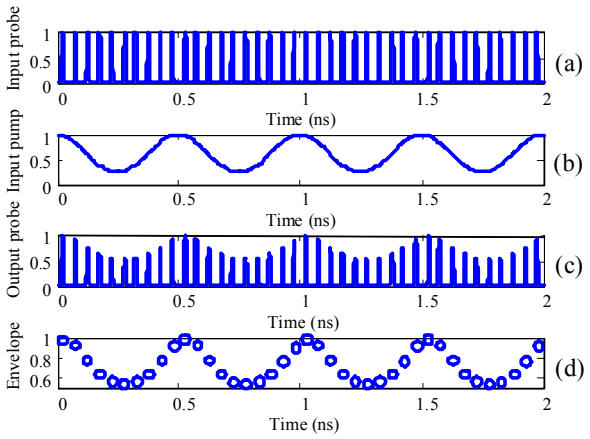

Fig. 4 Normalized powers of the (a) input probe light and (b) input pump light; normalized powers of the (c) output probe light and (d) output probe envelope.

pulse is achieved successfully. For calculation, the bias current of the SOA is set to 350 mW. The peak power of the probe light is 0.3 mW, and its repetition rate is 20 GHz. The pump light has the 4-mW peak power and 1-mW valley power, and its frequency is different from the probe light. The incident polarization angles are both at the degree of 45.

After that, the positions of the probe light and pump light are exchanged to achieve the sampling of the high frequency pulse to the analog signal. Figure 5(a) shows the sampling result, and it is obvious that there is a big distortion in the output probe light. When there is no time-varying input optical signal, the carrier concentration and photon density will reach a steady state of dynamic equilibrium in SOA's active region. But when there is a pulse light injection, this balance is broken, and the carrier will experience a slow recovery process to reach the stable state.

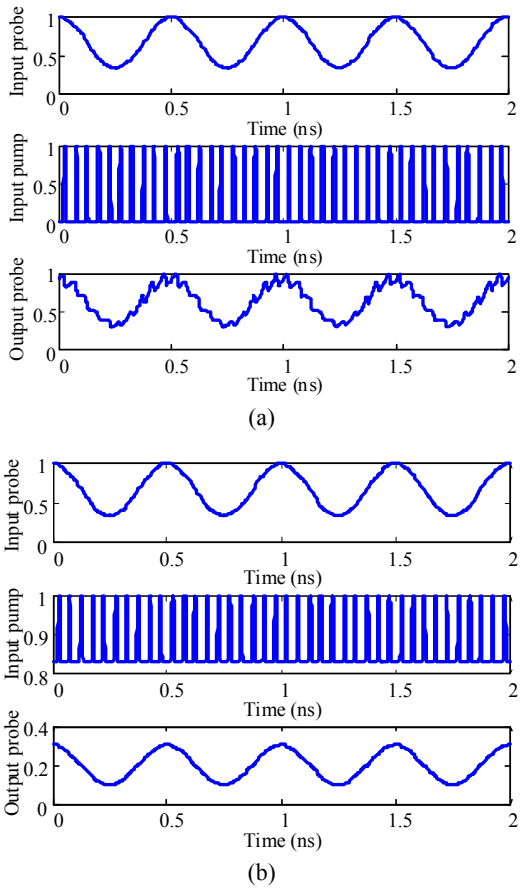

Fig. 5 Sampling results of exchanged probe and pump lights: (a) without holding light and (b) with holding light.

In order to reduce that distortion, we add a holding light to the pump light, and the improved sampling result is shown in Fig. 5(b). It is observed that holding light injection can improve the linearity of the all-optical sampling effectively, which is because suitable holding light power accelerates carrier recovery greatly, so it can speed up the response to the ultrafast signals and suppress signal distortion introduced by slow gain recovery to eliminate signal frontier overshoot. However, the disadvantage of this approach is that the gain will decline leading to negative impacts.

3.4 Linearity and efficiency of sampling

Taking into account the influence of the pulse width on the sampling results, we apply the Fourier curve to fit the pulse envelope of the 20-GHz sampling pulse of different pulse widths, and calculate the fundamental efficiency E_1 and k-order harmonic distortion D_k, and the correlation coefficient is near 0.99999. Due to that the harmonic distortion is mainly from the second harmonic, this paper mainly compares the values of E_1 and D_2 in the analysis. The band effect needs to be considered for the narrow pulse of less than 2-ps width, so we only analyze the case of a pulse width of several ps. The E_1 and D_2 values of different pulse widths of 1-G, 2-G, and 2.5-G analog signals are shown in Figs. 6(a) and 6(b), respectively. As can be seen from the figures, the sampling pulse width affects both the fundamental efficiency and second harmonic distortion, and has a nearly linear relationship. This is because of the impact of SOA carrier recovery time that when the sampling pulse width is narrower, the carrier recovery concentration is greater, and the obtained pulse value is greater after the SOA, so the fundamental efficiency is higher, and the second harmonic distortion is smaller.

We analyze the sampling performance of the analog signals of different frequencies. Each sampling pulse width is 6.5 ps, and the fitting

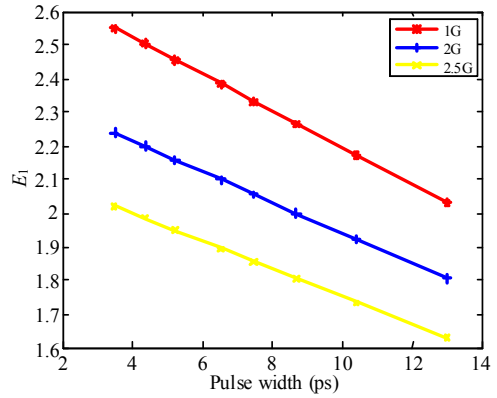

(a)

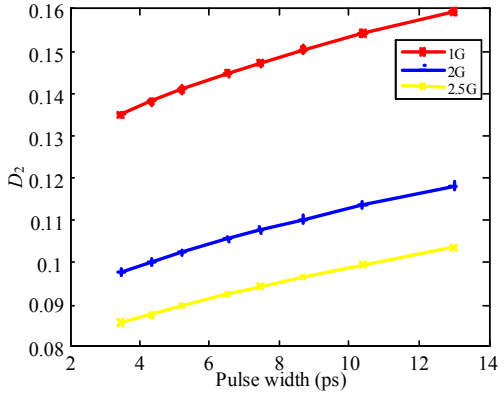

(b)

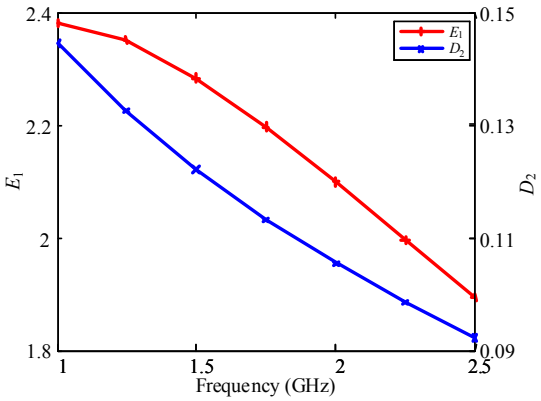

(c)

Fig. 6 Sampling linearity and efficiency: (a) E_1 of different pulse widths, (b) D_2 of different pulse widths, and (c) E_1 and D_2 of different frequencies.

correlation coefficient is near 0.99999. Figure 6(c) shows the corresponding value curves of E_1 and D_2, as can be seen from the figure, with an increase in the frequency, the second harmonic distortion decreases, but its fundamental efficiency also decreases. For the analog signals of the same power range, when the frequency is higher, the power difference between adjacent pulse sampling points is greater, and the carrier concentration change magnitude is bigger, so the second harmonic distortion is smaller. Affected by carrier recovery time, the signal with the lower frequency has greater carrier concentration difference between power peaks and troughs, and the obtained gain and its fundamental efficiency are higher. Thus, the analog signal frequency is higher, at the same time of getting better second harmonic distortion, the fundamental efficiency is sacrificed.

4. Conclusions

We construct a theoretical all-optical sampling model based on the nonlinear polarization rotation effect of the semiconductor optical amplifier and discuss the impact of the input light power, bias current, PDG, LEF, pulse width, and frequency on the sampling effect. The feasibility of the proposed scheme has been proved, and the process of all-optical sampling is achieved by simulation. We study the evaluation methods of all-optical sampling efficiency and linearity, and obtain the fundamental efficiency and second harmonic distortion to evaluate the sampling performance. The presented optical sampling method has an important role in promoting the application of optical sampling in the all-optical signal processing.

Acknowledgment

This work was supported by the National Natural Science Foundations of China (Grant No. 61378061 and 61575026).

References

[1] H. Lee, H. Yoon, Y. Kim, and J. Jeong, "Theoretical study of frequency chirping and extinction ratio of wavelength-converted optical signals by XGM and XPM using SOA's," *IEEE Journal of Quantum Electronics*, 1999, 35(8): 1213−1219.

[2] M. Jabbari, M. K. Moravvej-Farshi, R. Ghayour, and A. Zarifkar, "XPM response of a chirped DFB-SOA all-optical flip-flop injected with an assist light at transparency," *Journal of Lightwave Technology*, 2009, 27(13): 2199−2207.

[3] J. Kim, M. Laemmlin, C. Meuer, D. Bimberg, and G. Eisenstein, "Theoretical and experimental study of high-speed small-signal cross-gain modulation of quantum-dot semiconductor optical amplifiers," *IEEE Journal of Quantum Electronics*, 2009, 45(3): 240−248.

[4] C. Vagionas, D. Fitsios, G. T. Kanellos, N. Pleros, and A. Miliou, "All optical flip flop with two coupled travelling waveguide SOA-XGM switches," in *Conference on Lasers and Electro-optics*, San Jose, CA, pp. 1−2, 2012.

[5] G. Contestabile, M. Presi, and E. Ciaramell, "Multiple wavelength conversion for WDM multicasting by FWM in an SOA," *IEEE Photonics Technology Letters*, 2004, 16(7): 1775−1777.

[6] L. Ma, P. Ghelfi, M. Yao, F. Berizzi, and A. Bogoni, "Demonstration of optical sample parallelisation for high-speed photonic assisted ADCs," *Electronics Letters*, 2011, 47(5): 333−335.

[7] S. Fu, W. Zhong, P. Shum, C. Wu, and J. Q. Zhou, "Nonlinear polarization rotation in semiconductor optical amplifiers with linear polarization maintenance," *IEEE Photonics Technology Letters*, 2007, 19(23): 1931−1933.

[8] Y. Liu, Q. S. Zhang, S. J. Zhang, L. Huang, X. G. Tang, H. P. Li, *et al*., "High-speed all-optical sampling based on nonlinear polarization rotation in a semiconductor optical amplifier," *Photonics and Optoelectronic*, 2010, 6838: 1−3.

[9] T. Durhuus, B. Mikkelsen, C. Joergensen, S. L. Danielsen, and K. E. Stubkjaer, "All-optical wavelength conversion by semiconductor optical amplifiers," *Journal of Lightwave Technology*, 1996, 14(6): 942−954.

[10] K. E. Stubkjaer, "Semiconductor optical amplifier-based all-optical gates for high-speed optical processing," *Selected Topics in Quantum Electronics*, 2000, 6(6): 1428−1435.

[11] S. Fu, P. Shum, L. Zhang, C. Wu, and A. M. Liu, "Design of SOA-based dual-loop optical buffer with a 3×3 collinear coupler: guideline and optimizations," *Journal of Lightwave Technology*, 2006, 24(7): 2768−2778.

[12] P. Li, L. Jiang, J. G. Zhang, J. Z. Zhang, and Y. C. Wang, "Low-complexity TOAD-based all-optical sampling gate with ultralow switching energy and high linearity," *IEEE Photonics Journal*, 2015, 7(4): 1−8.